ELSEVIER

Spectrochimica Acta Part A 57 (2001) 843–858

SPECTROCHIMICA ACTA PART A

www.elsevier.nl/locate/saa

Mid- and far-infrared spectroscopic studies of the influence of temperature, ultraviolet photolysis and ion irradiation on cosmic-type ices

M.H. Moore [a,*], R.L. Hudson [b], P.A. Gerakines [c,1]

[a] *Code 691, Astrochemistry Branch, NASA/Goddard Space Flight Center, Greenbelt, MD 20771, USA*
[b] *Department of Chemistry, Eckerd College, St. Petersburg, FL 33733, USA*
[c] *Code 691, Astrochemistry Branch, NRC/NASA Goddard Space Flight Center, Greenbelt, MD 20771, USA*

Received 21 June 2000; received in revised form 26 September 2000; accepted 26 September 2000

Abstract

Infrared (IR) studies of laboratory ices can provide information on the evolution of cosmic-type ices as a function of different simulated space environments involving thermal, ultraviolet (UV), or ion processing. Laboratory radiation experiments can lead to the formation of complex organic molecules. However, because of our lack of knowledge about UV photon and ion fluxes, and exposure lifetimes, it is not certain how well our simulations represent space conditions. Appropriate laboratory experiments are also limited by the absence of knowledge about the composition, density, and temperature of ices in different regions of space. Our current understanding of expected doses due to UV photons and cosmic rays is summarized here, along with an inventory of condensed-phase molecules identified on outer solar system surfaces, comets and interstellar grains. Far-IR spectra of thermally cycled H_2O are discussed since these results reflect the dramatic difference between the amorphous and crystalline phases of H_2O ice, the most dominant condensed-phase molecule in cosmic ices. A comparison of mid-IR spectra of products in proton-irradiated and UV-photolyzed ices shows that few differences are observed for these two forms of processing for the simple binary mixtures studied to date. IR identification of radiation products and experiments to determine production rates of new molecules in ices during processing are discussed. A new technique for measuring intrinsic IR band strengths of several unstable molecules is presented. An example of our laboratory results applied to Europa observations is included.

Keywords: IR spectroscopy; Condensed-phase; Ices; Energetic processing; Radiation chemistry; UV photolysis

1. Introduction

One of the major questions in the formation and evolution of condensed-phase molecules in interstellar environments is their production, which may proceed either via grain-surface chem-

* Corresponding author. Fax: +1-301-2860440.
E-mail address: ummhm@lepvax.gsfc.nasa.gov (M.H. Moore).
[1] Present Address: Department of Physics, University of Alabama at Birmingham, 1300 University Blvd., Birmingham, AL 35294.

1386-1425/01/$ - see front matter
PII: S1386-1425(00)00448-0

istry or by accretion of simple molecules with subsequent processing by cosmic rays, UV photons, or a combination of both. Although research on grain-surface reactions represents the future direction of several laboratories, our experiments have focused on the processing of ices by protons and UV photons. The goal is to study the infrared spectra of key molecules and mixtures of molecules, and from those experiments identify new species formed during processing, and to measure the yield of major products. Many experiments also apply to ices in solar system environments when the ice composition, temperature, or bombarding flux is varied to simulate what is known about each icy-satellite, planetary, or cometary environment.

Laboratory experiments on UV-photolyzed and ion irradiated ices lead to the formation of many complex organic molecules, and seem to be representative of processes occurring in space. However, the exact nature of complex space environments is a major question connected to the correct dose of energetic processing in different regions. The flux of cosmic-ray ions onto the surface of a cometary nucleus stored for 10^9 years in the Oort cloud (or Kuiper belt) or the flux of ions onto the surface of the Galilean satellites is more accurately modeled than the cosmic-ray flux encountered in various molecular clouds. Possible evidence for processing in interstellar ices includes the so-called 'XCN' feature at 4.62 μm [1–3], the 6.8 μm band [4,5], and the triple peak structure of the bending mode of CO_2 at 15.2 μm indicative of thermally-processed $H_2O + CO_2 + CH_3OH =$ 1:1:1 ice seen towards a number of massive protostellar sources [6,7]. Analysis of band shapes of CO_2 in many sources observed by the Infrared Space Observatory (ISO) reveals that CO_2 exists in both polar (H_2O and CH_3OH) ice matrices and in non-polar ices such as N_2, CO, or O_2 [6,8]. Another observational clue supporting thermal processing is the interstellar (IS) signature of the apolar CO_2 ice component which resembles that of annealed CO_2, rather than CO_2 condensed at 10 K. Evidence for energetic processing of cometary ices prior to accretion comes from the detection of abundant C_2H_6 in comet Hyakutake [9]. An abundance of C_2H_6 comparable with that of CH_4 implies that the ices did not originate in a thermochemically-equilibrated region of the solar nebula, but were produced by UV or radiation processing of interstellar icy grain mantles (see [10,11] for discussions of relevant experiments). Evidence for processing on the Jovian satellite, Europa, comes from the detection of H_2O_2 formed by ion bombardment of its H_2O-dominated surface ice [12] (for discussions of relevant experiments see [13]).

The bulk of solar system spectroscopic observations are obtained at visible and near-IR wavelengths (0.4–5 μm) since icy surfaces are observed in reflection or emission. However, laboratory experiments that focus on the identification of molecules, use the mid-IR (2–20 μm) spectral region. The fundamental vibration bands found in the mid-IR are much stronger than their overtones found in the near-IR, and are, therefore, more accurate indicators of molecular abundances in laboratory experiments. The far-infrared region (20–100 μm) contains absorptions due to intermolecular vibrations (lattice vibrations) and is often used for structural information. In the laboratory, good quality transmission spectra of thin ice films are used to identify molecular positions, and to calculate intrinsic band strengths of molecules. The detailed comparison of these spectra to observations requires modeling to account for effects such as grain size and shape distribution (see discussions in [14]).

1.1. Nature of radiation environments

In IS space, the galactic cosmic-ray environment is thought to have an isotropic flux which, on average, has been the same throughout the age of the solar system, 4.6×10^9 years. It is estimated that cosmic rays are 87% protons, 12% helium nuclei, and 1% heavier nuclei. The IS electron cosmic-ray flux is a factor of 10 to 100 times smaller than the proton flux for energies below 100 MeV. Radiation processing of ices by cosmic rays is dominated by protons, whose intensity is largest in the low MeV range and whose energy spectrum decreases with a power law index of 2.5 at higher energies.

The energy deposited per cm as a proton moves through a solid (the stopping power) has a maximum value for proton energies near 0.1 MeV. A typical 1 MeV proton has a stopping power of ~ 300 MeV cm^2 g^{-1} and a range near 23 μm in H_2O ice. In an ice, MeV protons cause numerous excitations and ionizations and produce many secondary electrons, which cause additional nearby ionizations. See Moore [15] and references therein for a more detailed discussion of cosmic-ray interactions with solids. Although the flux of low energy ($\sim$MeV) galactic cosmic-ray protons cannot be directly measured, it is estimated from observations of H_3^+ absorption and $H^{13}CO^+$ emission lines, combined with models of the temperature and density structure of the sources. The average cosmic-ray ionization rate is $2.6 \pm 1.8 \times 10^{-17}$ s^{-1} with variations of order 50% on a scale of $\approx$10,000 light years [16]. The inferred flux of low energy MeV protons is calculated from the ionization rate using an appropriate ionization cross-section. In the diffuse IS medium, the estimated flux range is from about 1 to 10 cm^{-2} s^{-1}. A flux of 1 MeV protons of 10 cm^{-2} s^{-1} (1×10^7 eV cm^{-2} s^{-1}) is used by Strazzulla and Johnson [17] for calculations of energy deposited in materials exposed to galactic cosmic-ray environments.

UV photons are also present in space environments, and those with wavelengths below ~ 200 nm cause ice photochemistry. Interstellar UV photons (mostly Lyman-α) are produced primarily by hot O and B stars, and the estimated number density of these sources results in a calculated intensity of 9.6×10^8 eV cm^{-2} s^{-1} between 91 and 180 nm. UV photons are absorbed in a single excitation or ionization event. In H_2O ice, with $\rho = 1$ g cm^{-3}, the UV transmission drops to 37% in 0.15 μm assuming a UV cross-section of 2×10^{-18} cm^2 from Okabe [18].

1.2. Effects of radiation environments

1.2.1. Interstellar ices

IS icy grain mantles (~ 0.02 μm thick) are subjected to both Lyman-α UV photons and cosmic rays, but since icy grains can exist within molecular clouds of varying gas and dust densities, the UV contribution varies. Models predict that in cold dark clouds (10–20 K) dust shields the interior ices from IS UV photons. However, cosmic ray induced fluorescence of molecular hydrogen produces UV inside the cloud. The energy dose from this internal UV source is thought to be similar in value to the energy contribution from the incoming cosmic rays. In cold diffuse clouds (~ 100 K), there is less UV attenuation and the dose due to the IS radiation field is orders of magnitudes greater than the dose from cosmic rays. Total doses for ices in these different regions for different time scales are summarized in Table 1.

1.2.2. Comets

Radiation modification of ices in comets can occur while they are stored in the Kuiper Belt or the Oort Cloud, where the radiation environment is dominated by cosmic-ray protons. It is estimated that the total dose accumulated in the upper 10 cm of cometary ice is larger than 150 eV mol^{-1} when the veneer of heavily UV-processed ice is included. However, deeper layers accumulate smaller ion doses and no UV processing, so the greatest modification takes place in the surface material of comets. Table 1 also summarizes current ideas of cosmic-ray doses in comets.

1.2.3. Satellites

Radiation modification of ices on outer solar system objects in some cases is dominated by the local magnetospheric radiation environment instead of galactic cosmic rays. For example, the icy Galilean satellites experience an average magnetospheric Jovian energy flux of 4×10^{13} eV cm^{-2} s^{-1} from e^-, p^+, O^{n+}, and S^{n+}, which is greater than the energy flux from galactic cosmic rays [22]. UV photochemistry plays a diminished role in these ices, since the flux from solar photons with energies greater than 6 eV is only 1% of the magnetospheric flux. Moreover, the contribution of UV products to the total abundance of observed molecules on these icy surfaces is likely to be insignificant because IR observations sample the top ~ 50 μm of the surface, whereas, UV photons only process the top 0.2 μm. Any chemical model of the abundance of radiation products on a dynamic icy surface needs to include the

Table 1
Predicted UV photon (E ≈ 10 eV) and 1 MeV proton fluxes in diffuse and dense IS cloud regions are used to calculate absorbed energy in 0.02 μm ice coated-grains and in the icy layers of a comet nucleus[a]

	UV			Protons		
Resident time of ices in region (years)	Flux 10 eV photon (eV $cm^{-2}s^{-1}$)	Energy absorbed (eV $cm^{-2}s^{-1}$)	Energy dose (eV per molecule)	Flux 1 MeV p^+ (eV $cm^{-2}s^{-1}$)	Energy absorbed (eV $cm^{-2}s^{-1}$)	Energy dose (eV per molecule)
IS ices in cold diffuse clouds	9.6×10^{8}	5×10^{8}		1×10^{7}	1.2×10^{4}	<1
10^5		(0.02 μm mantle)	1×10^{4}		(0.02 μm mantle)	3×10^{1}
10^7			1×10^{6}			3×10^{3}
10^9			1×10^{8}			
IS ices in cold dense clouds	1.4×10^{4}	1.7×10^{3}		1×10^{6}	1.2×10^{3}	
		(0.02 μm mantle)			(0.02 μm mantle)	
10^5			<1			<1
10^7			4			3
10^9			4×10^{2}			3×10^{2}
Cometary ices in Oort cloud	9.6×10^{8}	9.6×10^{8}		ϕ(E)		
4.6×10^{9}						~150 (0.1 m)
			2.7×10^{8}			~55–5 (1–5 m)
			(0.15 μm layer)			
						<10 (5–15 m)
Typical laboratory experiment	8.6×10^{14}	8.6×10^{14}	14	7×10^{10}	1×10^{16} (5 μm)	9
		(0.26 μm)				
4.6×10^{-4}						

[a] The absorbed energy dose from 1 MeV cosmic-ray protons is calculated assuming a 300 MeV cm^2 g^{-1} stopping power and assuming that protons deposit energy in both the entrance and exit ice layer of an ice coated grain. The ice density is assumed to be 1 g cm^{-3}. Calculations for the IS environments are based on Jenniskens et al [19], Strazzulla and Johnson [17], Wdowiak [20] and Duley and Williams [21]. An energy dependent flux, ϕ(E), is used to calculate the resulting energy dose at different depths in a comet nucleus (for details see Strazzulla and Johnson [17] and references therein). Typical UV and proton fluxes and doses measured in our laboratory are shown in the last line for comparison

effects of removal processes (e.g. sputtering and thermal sublimation) and burial mechanisms (e.g. impact gardening). Impact gardening on solid solar system surfaces can mix surface material on a short time scale to depths greater than the penetration depth of bombarding ions.

1.3. Inventory of condensed-phase molecules

A typical inventory of molecules in IS ice mantles is represented by the spectrum recorded by ISO of a source called NGC 7538 IRS9 [23]. One surprising observation about this spectrum is that unprocessed laboratory ice mixtures can explain most of the features. The only exceptions are the so-called 'XCN' feature at 4.62 μm and the unidentified 6.8 μm band, which may be indicators of energetic processing [1–5].

H_2O is the dominant condensed-phase molecule in the NGC 7538 IRS9 spectrum and in other cosmic ices. A clue to the ice temperature comes from the spectral identification of the ice phase. Evidence for both amorphous and crystalline phase H_2O in different IS sources is discussed in Section 3. Observations of most icy solar system surfaces, including the rings of Saturn, reveal that H_2O is crystalline [24]. In comet Hale–Bopp, evidence for amorphous phase icy grains of H_2O was detected in near-IR spectra based on the absence of the 1.65 μm absorption feature [25].

Table 2 lists the molecules observed in IS ices, cometary ices, and ices on satellites and Pluto. Mid-IR laboratory spectra of the majority of the molecules in Table 2 are known in the condensed-phase, as are the spectra of each mixed with solid H_2O. In general, less information is available for ices containing sulfur, for molecules such as HCN and for N_2.

2. Experimental

Details concerning our laboratory setup and techniques are already in print [29,30,32]. IR spectra of thin ice films are measured before and after ion bombardment or UV photolysis to identify ratiation products and to determine changes in spectral band strength with dose or with thermal processing. Fig. 1 is a schematic of our experimental arrangement. Ices were formed by slow condensation from appropriate vapor-phase mixtures at room temperature onto a cold (16 K) polished aluminum mirror (area 5 cm^2) mounted on the tail of a cryostat. A vacuum of about 10^{-8} torr was maintained within the cryostat. A heater provided the capability of maintaining samples at temperatures between 16 and 300 K. Ice thicknesses were on the order of a few micrometers for ion irradiation experiments, and were measured using a laser interference system assuming an index of refraction of 1.3 for H_2O-dominated ices [32]. Deposition rates were roughly 1–5 μm h^{-1}. Ice thicknesses for UV-photolysis experiments were as small as 0.1 μm. An FTIR spectrometer was used to record mid-IR (4000–400 cm^{-1}) spectra with a resolution of 4 or 1 cm^{-1}, depending on the nature of the experiment. Since the IR beam passed through the ice before and after reflection at the ice-mirror interface, this IR measurement is called transmission-reflection-transmission (TRT).

Table 2
Molecules detected in the solid phase as IS ice mantles and on the surfaces of several planetary satellites and Pluto[a]

Sources	Detected condensed-phase molecules
IS molecular cloud, NGC 7538 IRS9[b]	H_2O, CO_2, CO, NH_3, CH_3OH, CH_4, OCN^-, $HCOO^-$
Comet Hale–Bopp[c]	H_2O, CO, CO_2, CH_3OH, H_2S, H_2CO, CH_4, NH_3, C_2H_2, C_2H_6, OCS, CS_2, SO_2, SO, HNCO, HCOOH, $HCOOCH_3$, HCN, CH_3CN, H_2CS, HC_3N, NH_2CHO, S_2, HNC
Ices on satellites and Pluto[d]	H_2O, H_2O_2, CO_2, CO, CH_4, O_2, O_3, N_2, NH_3, SO_2, SO_3, H_2S, NH_3

[a] Ices on comets are inferred from the identification of parent molecules in emission spectra of the comae (with the exception of H_2O ice detected in comet Hale–Bopp [24]).

[b] See reviews; Tielens and Whittet [23] and Gibb et al [26].

[c] Icy material from the comet nucleus sublimes releasing these gas-phase molecules into the coma. For abundances see review by Crovisier [27].

[d] See reviews by Cruikshank et al [28] and Schmitt et al [14].

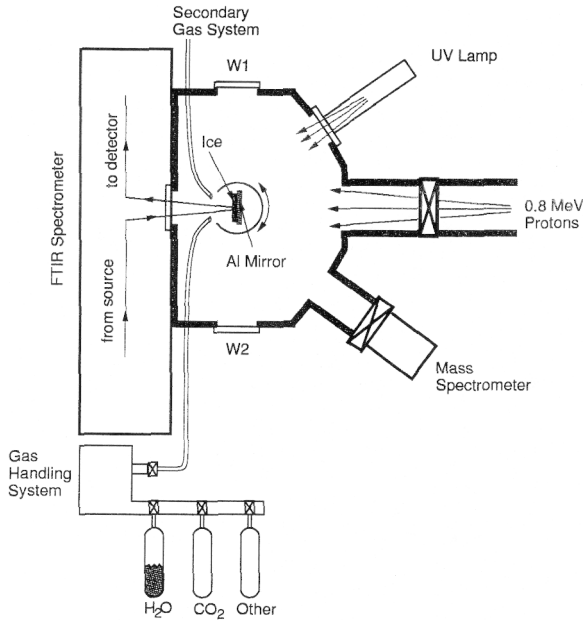

Fig. 1. Schematic of laboratory set-up.

Far-IR measurements (500–100 cm^{-1}) reported in this paper were recorded in conventional transmission by repositioning the spectrometer so that the IR beam passed through polypropylene windows, located at W1 and W2, and through the ice formed on a silicon substrate. Temperature-sensitive bands in the p-type silicon were removed from each spectrum by ratioing with a background spectrum at the same temperature. The silicon substrate provided a better thermal connection to the cryostat than a polyethylene substrate used in measurements by Smith et al. [33], Hudgins et al. [32], or Schmitt et al. [14]. Transmission measurements avoided possible errors from added signals due to front surface reflections and internal reflections that appear in the TRT technique.

To process a sample by ion bombardment, the ice was rotated to face a beam of 0.8 MeV protons generated by a Van de Graaff accelerator. Typically, a beam current of 0.1 μA and incident fluences of 10^{13}–10^{15} protons cm^{-2} was used. Incident fluences were converted into eV mol^{-1} by way of the stopping power of the energetic proton, which in turn required knowing the ice density. However, since the density was largely unknown, we assumed a value of 1 g cm^{-3} for H_2O-dominated ices. For pure water, a fluence of 1×10^{15} protons cm^{-2} corresponded to 11.4 eV mol^{-1}. For mixed ices, weighted averages of the stopping powers for each initial component were used. Details about these techniques and calculations are given in Hudson and Moore [30] and Moore and Hudson [10]. Since the incident 0.8 MeV protons had a range of 16 μm [34], they penetrated each ice sample and came to rest in the aluminum mirror. The bombarding proton was not implanted into the ice. Ionizations and excitations caused by the incident radiation initiated the radiation chemistry pathways.

A microwave-discharge hydrogen flow lamp that produced primarily Lyman-α photons ($\lambda =$ 121.6 nm, $E = 10.2$ eV; see e.g. Warneck [35]) was interfaced with the vacuum chamber as shown in Fig. 1. The lamp discharge was separated from the vacuum system by a UV-transmitting lithium fluoride window. The lamp's flux at the ice was calculated to be 8.6×10^{13} photons cm^{-2} s^{-1} (for $\lambda < 185$ nm) by measuring the $O_2 \rightarrow O_3$ conversion rate during the photolysis of pure O_2 ice at 18 K. Details of these calculations are given by Gerakines et al. [31]. To ensure UV processing throughout the bulk of the ice, samples were less than 0.5 μm thick. Thicker processed samples could be formed by simultaneously depositing and photolyzing.

3. Results and discussion

3.1. Far-IR spectra of water ice

H_2O ice and H_2O-dominated icy mixtures are important constituents of IS grain mantles, of comets, and many of the outer planetary satellites. The far-IR spectrum of H_2O is of interest to astronomers since distinct lattice vibrations in this region reveal the ice phase. For the first time, a continuous view of IR sources from 2.5 to near 200 μm was possible with the wide spectral coverage provided by ISO. Although the spectra of cold molecular clouds show many far-IR signatures, they often have blended features of various

silicate grain mineralogies with (in some cases) water ice. Dartois et al. [36] reported evidence for the 44-μm band of crystalline phase H_2O ice in absorption toward IRAS 19110 + 1045 and in another source, IRAS 18316-0602, identified amorphous phase H_2O. Waters [37] detected both the 44 μm and 62 μm bands of ~65 K crystalline ice toward the source HD 161796.

Identifying water-ice's phase in a particular line of sight may help determine its temperature history in an IS environment. H_2O is amorphous, if condensed at temperatures below ~100 K, crystalline H_2O forms at higher temperatures. Amorphous H_2O irreversibly crystallizes when warmed. There is a dramatic difference between the far-IR spectrum of amorphous H_2O, with a featureless broad absorption peak near 45 μm, and crystalline H_2O with two peaks (the so-called 44 and 62 μm bands). Although a good observational clue, the ice phase may not be sufficient to determine the temperature or thermal history of the ice since crystalline ice can be amorphized with sufficient energetic processing (ions and UV photons) at temperatures below ~50 K. This effect cannot be excluded until the dose of energetic processing is better known in IS regions.

The far-IR spectrum of H_2O ice also shows changes in peak position and intensity with temperature. The peak position of amorphous H_2O shifts to smaller wavenumbers as the temperature increases. After the irreversible crystallization of H_2O at 160 K, the peak near 222 cm^{-1} (45 μm) shifts to larger wavenumbers (reversibly) with cooling. Fitting an IS H_2O ice band ultimately depends on appropriate laboratory spectra and optical constants. Far-IR band positions and band profiles for H_2O between ~14–160 K have been examined by Moore and Hudson [38], Smith et al. [33], and Schmitt et al. [28]; absorbance values were published by Schmitt et al. [14], and Coustenis et al. [39], and optical constants by Hudgins et al. [32].

Here we report our best illustration of the combined effects of temperature and thermal history on the bands of water ice. Fig. 2a shows the spectrum of water deposited at 14 K and warmed to 30, 80, 100, 120, 140 and 160 K. The spectrum at 14 K had a maximum absorbance of 0.37 at 218 cm^{-1}. Using the optical constants of Hudgins et al. [32] and our known deposition time, this corresponds to a thickness of 7.2 μm and a deposition rate of 11 μm h^{-1}. Fig. 2b shows the spectrum of water deposited at 160 K and cooled to 140, 120, 100, 80, 30 and 14 K. The spectrum at 160 K had a maximum absorbance of 0.75 at 225 cm^{-1}. Using our known deposition time and the optical constants of Bertie et al. [40], or comparing with the measurements of Smith et al. [33], a thickness of ~5 μm was estimated for the ice, corresponding to a deposition rate of ~5 μm h^{-1}. A third set of data, shown in Fig. 2c, was obtained when water was deposited at 140, 120, 100, 80 and 30 K. The complete set of data in Fig. 2 is available at: www-691.gsfc.nasa.gov/cosmic_ices. Fig. 3a plots the reversible changes we measured in the 44 and 62 μm peak positions of crystalline water (deposited at 160 K) with temperature. Also shown is the data of Smith et al. [33] and Schmitt et al. [14]. This plot compares three very similar data sets recorded in three different laboratories. Overall, the plot shows comparable results were obtained and differences are within the spectral resolution (4 cm^{-1} for Smith et al. [33] and 2 cm^{-1} for Schmitt et al. [14]). In Fig. 3b we have included the 44/62-μm peak height ratio of crystalline water at different temperatures. These laboratory results can be fitted to observations in order to determine ice temperature (in the absence of any processing effects) and to search for minor species whose spectral signatures may be present in the sub-structure of the 44 or 62 μm H_2O bands.

3.2. First laboratory comparison of ion irradiation with UV photolysis-carbonic acid

When considering ices in different space environments and the variety of molecules present, it is obvious that a complex array of radiation- and photo-chemistries may occur. An unsolved problem in laboratory astrophysics is the quantitative comparison between ion bombardment and UV photolysis of cosmic-type ices. In the absence of relevant experiments, it is usually assumed that UV photolysis and ion irradiation produce identical results. Therefore, studies to determine whether the action of photons and energetic particles form the same major products, with the same efficiency, are warranted.

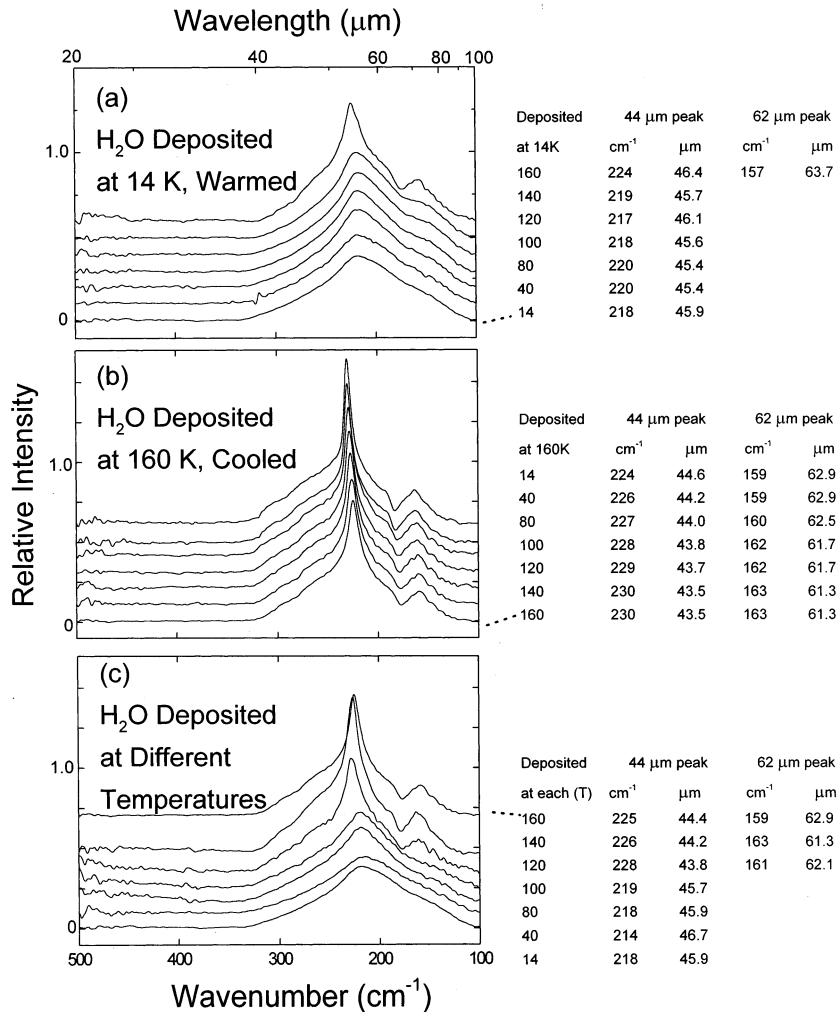

Fig. 2. Far-IR spectra of H_2O and tabulated peak positions. (a) H_2O deposited at 14 K and warmed; (b) H_2O deposited at 160 K and cooled; (c) H_2O deposited at different temperatures.

We have completed the first set of experiments to compare the effects of proton irradiation and UV photolysis on ices [31]. The formation of H_2CO_3 by proton bombardment of $H_2O + CO_2$ ice mixtures has been shown in previous experiments [41]. Now, H_2CO_3 has also been identified in photolyzed $H_2O + CO_2$ ices [31]. Crystalline-phase H_2CO_3 is less volatile than H_2O, and its IR signature is measured after slow warming of the ice to near 200 K. Fig. 4 shows the spectrum of $H_2O + CO_2$ and the carbonic acid formed after proton bombardment and after photolysis. Since the formation of H_2CO_3 by UV photolysis is limited to the penetration depth of the photons, its IR identification was not secured until a careful set of experiments were completed in which ice samples were created by simultaneous condensation and UV photolysis of the $H_2O + CO_2$ gas[2].

[2] Simultaneous condensation and UV photolysis is a technique used to increase the amount of UV exposure in the bulk of the ice. While gas-phase reactions during condensation could occur, observed photolysis products in the 'condense and then photolyze' case are identical to those in the 'simultaneous condensation and photolysis' case.

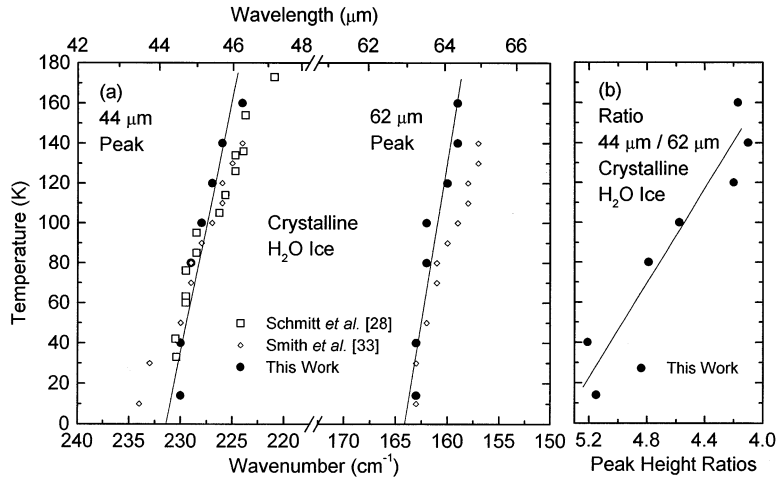

Fig. 3. (a) Change in the 44 and 62 μm peaks of crystalline H_2O ice as a function of temperature. Linear least-square fit to our laboratory data is compared with data from two other laboratories. (b) 44/62 μm peak height ratio of crystalline H_2O ice as a function of temperature.

Determination of the intrinsic band strength of H_2CO_3 ($A(H_2CO_3)$) is discussed in Section 3.3. Using $A(H_2CO_3)$, the formation rates of H_2CO_3 as a function of dose, shown in Fig. 5, seem to be independent of the type of energetic processing. CO, the other major product, is also formed at a rate independent of the processing type. $A(H_2CO_3)$ and the change in the H_2CO_3 band area as a function of time due to sublimation lead to a vapor pressure at 250 K of 1.5×10^{-7} torr for crystalline H_2CO_3. The corresponding vapor pressure for crystalline H_2O at 250 K is 1 torr.

Recent experiments with $H_2O + CH_3OH$, $H_2O + CH_3OH + CO_2$, and $H_2O + CH_4$ ices also show the same rate of formation of major products independent of the two types of processing (spectra not shown). There is one difference in that the formate ion, $HCOO^-$, seen in ion bombarded $H_2O + CH_3OH$ and $H_2O + CH_3OH + CO_2$, is not detected when the mixture is photolyzed. This is discussed further in the next section. It is possible that other differences will be seen e.g. for molecules with high dissociation energies such as CO (11.1 eV) and N_2 (9.8 eV), since MeV protons may have a much larger impact on these molecules than 10.2 eV photons and allow them to more effectively take part in the chemical reactions. Relevant experiments are currently in progress.

3.3. Band strengths of unstable molecules and radicals

The intrinsic band strength of a condensed phase molecule can be used to determine its concentration, or rate of formation in irradiated ices and to assess its role in a reaction pathway. There are a few reliable measurements of absolute band strengths (A cm mol^{-1}, intrinsic absorbances) of condensed-phase molecules, but too often the information is limited by temperature, wavelength, or matrix. Standard measurement methods involve condensing an ice of measured thickness whose composition and density are (poorly) known. These parameters can be used to determine the column density (N) of an individual molecular component in an ice. Values of the band area and N, lead to an A-value:

$$A(v_1,v_2) = \frac{1}{N}\int_{v_1}^{v_2} ln(I_0/I)dv$$

An alternate procedure, applied when the intrinsic band strength is unknown, has been to use the gas-phase value, but this can lead to errors because band strengths can depend on the molecular environment. For example, the 1300 cm^{-1} band of CH_4 has $A_{gas} = 5.23 \times 10^{-18}$ cm mol^{-1} [42], $A_{solid} = 3.8 \times 10^{-18}$ cm mol^{-1} for pure CH_4

ice and $A_{solid} = 4.7 \times 10^{-18}$ cm mol^{-1} for CH_4 in an H_2O matrix [32]. The affect of the environment is often band dependent as well (e.g. stretch, bend, or liberation), e.g. $A_{solid}/A_{gas} = 0.62$ for the ν_5 band of C_2H_2, but this ratio is 5.5 for the ν_3 band [43].

Properly determined laboratory values of A for condensed-phase molecules in matrices dominated by H_2O are relevant for many IS and planetary ice observations. Standard methods, however, cannot be used to measure the A-values of unstable species formed in some irradiation experiments. Instead the A-value of some unstable species can be determined, if they photodissociate into a product, P, whose intrinsic band strength is known. The A-value of the unstable species is determined by observing the balance between its disappearance and the formation of P. Two examples are discussed — H_2CO_3, which is unstable at STP, and the radical HCO, which is stable in H_2O matrices to $\sim$100 K on laboratory time scales.

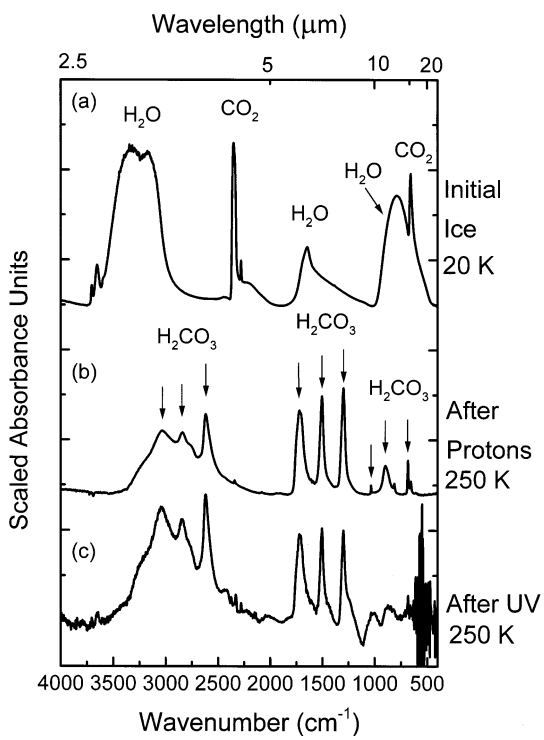

Fig. 4. Mid-IR spectra of $H_2O + CO_2$ before processing (a) is compared with (b) H_2CO_3 at 250 K formed after warming proton irradiated $H_2O + CO_2$ at 20 K and (c) H_2CO_3 at 250 K formed after warming UV processed $H_2O + CO_2$ at 20 K.

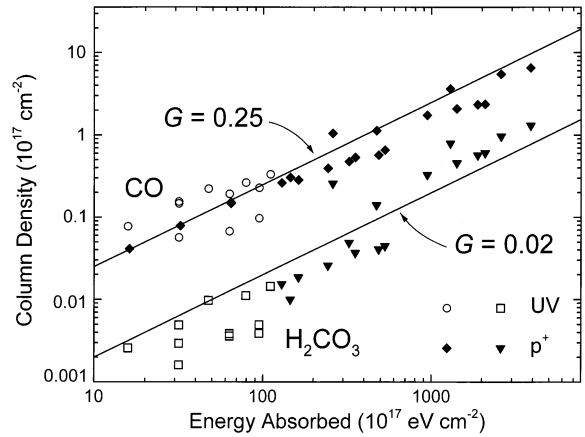

Fig. 5. Change in the column density of CO and H_2CO_3 as a function of the energy absorbed during processing. Data are fitted with linear least-square lines whose slopes are equal to the number of molecules formed per 100 eV, G. $G(CO) = 0.25$ and $G(H_2CO_3) = 0.02$.

Since both H_2O and CO_2 have been detected in different astrophysical environments (IS, comets, icy Galilean satellites, Triton and Mars), it is possible that H_2CO_3 may form as a radiation product. Predicting the abundance of H_2CO_3 in a cosmic ice is based on its calculated formation rate in laboratory ices, a rate that requires knowing the intrinsic band strength. We determined $A(H_2CO_3)$by measuring its IR spectrum during photodissociation into CO_2, a product with a known band strength. When pure H_2CO_3 is photolyzed, $H_2CO_3 + h\nu \rightarrow H_2O + CO_2$, and since the intrinsic IR band strength of CO_2 has already been determined (pure CO [44]; pure CO_2 [45]; H_2O-dominated mixtures with CO and CO_2 [46]), the column density of CO_2 can be calculated. The number of CO_2 molecules produced equals the number of H_2CO_3 molecules destroyed. CO is also taken into account once a significant amount is created from the CO_2. Fig. 6b shows three bands of H_2CO_3 at 20 K before and after photolysis. From the decrease in the H_2CO_3 bands, and the increase in the CO_2 band area shown in Fig. 6a, A(1485 cm^{-1}, H_2CO_3) $\sim 6 \times 10^{-17}$ cm mol^{-1} is calculated [31].

The second example, is the 1853 cm^{-1} band of the formyl free radical (HCO) identified in photolyzed $H_2O + CO$ and $H_2O + H_2CO$ ices [47]. We

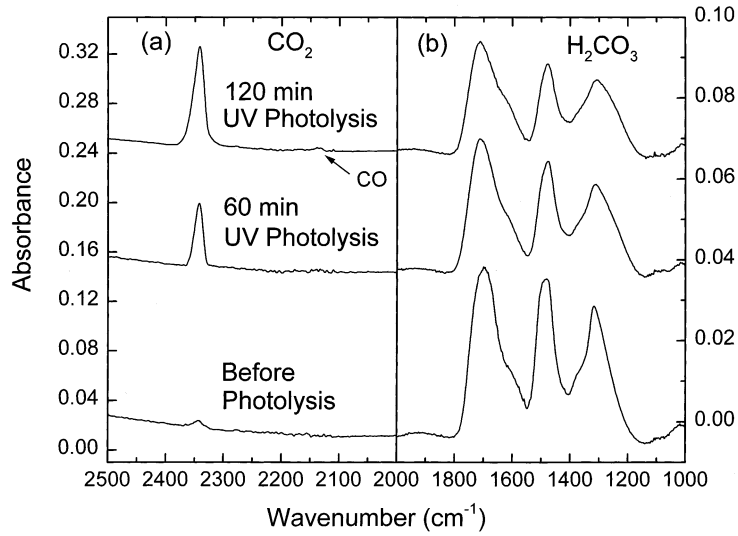

Fig. 6. During UV photolysis of pure H_2CO_3 at 20 K, $H_2CO_3 \rightarrow H_2O + CO_2$. Decreases in the band areas of H_2CO_3 occur as CO_2 is formed.

observe a similar feature in proton-bombarded ices. HCO formation is the first step in the production of H_2CO, CH_3OH and other organic molecules in photolyzed or ion-bombarded ices containing H_2O, and in grain-surface reactions, by the addition of hydrogen atoms. Predicting the abundance of HCO in cosmic ices is based on its formation rate in our laboratory ices, a value requiring $A(H_2CO_3)$. To determine A(HCO), we exposed an irradiated $H_2O + H_2CO$ ice, showing the HCO band, to unfiltered visible light from a 60 W tungsten lamp. Fig. 7b shows the decrease in absorbance of the HCO band over a few hours along with an increase in CO, Fig. 7a. These observations show that photobleaching causes $HCO \rightarrow H + CO$; the number of CO formed equals the number of HCO destroyed. From the decrease in HCO, the corresponding increase in the CO band, at 2137 cm^{-1}, and CO's known band strength (1.7×10^{-17} cm mol^{-1} [48])[3], we have calculated a value of $A(HCO) \approx 2.1 \times 10^{-17}$ cm mol^{-1}. This value can be used to determine an upper limit for the abundance of the HCO radical, which has not been detected in ISO observations.

[3] If $A(CO) = 1.1 \times 10^{-17}$ cm mol^{-1} [46], then $A(HCO) = 1.4 \times 10^{-17}$ cm mol^{-1}

3.4. Identification of new species after energetic processing

IR spectroscopy is the key to identifying new species formed after energetic processing of ices. Spectroscopy is also used to track the products retained in the ice during warming and to monitor the formation of new bands due to any reactions (e.g. radical, acid-base) that occur. Some new species are more volatile than the original parent molecule (e.g. CO synthesis from CO_2) and some are less volatile (e.g. ethylene glycol, $C_2H_4(OH)_2$, from CH_3OH). The motivation for our choice of experiments comes from astrophysical problems.

We have examined many icy mixtures using different concentrations of hydrocarbons to determine if yields of C_2H_6 from CH_4 due to dimerization were similar to yields of C_2H_6 from C_2H_2 due to H-addition reactions [11,10]. These experiments were motivated by the detection of C_2H_6, CH_4 [9], and C_2H_2 [49] in Comets Hyakutake and Hale–Bopp [50]; the surprisingly high abundance of C_2H_6 relative to CH_4 suggested solid-phase UV or radiation processing of cometary ices prior to accretion [9].

In a different set of experiments, we showed that IR spectroscopy of radiation-processed icy mixtures of H_2O and CO formed HCO, H_2CO,

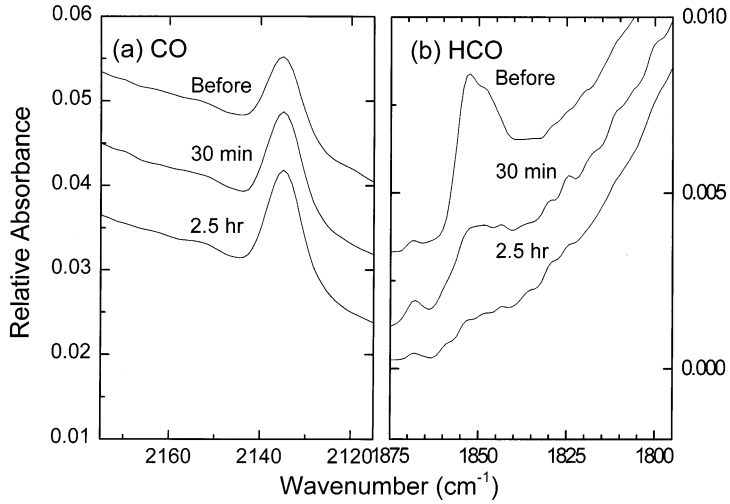

Fig. 7. Photobleaching the HCO radical at 20 K forms CO.

HCOOH, and CH_3OH [51]. We used isotopic labeling to study an H-atom addition mechanism for the low-temperature solid-phase reaction sequence from CO to CH_3OH. In the next phase of experiments, we measured the formation rate of CH_3OH, which is relevant to IS ices since an efficient pathway for its formation has not been demonstrated. Our experiments were the first to quantify a relatively high conversion rate of $CO \rightarrow CH_3OH$ in ion bombarded $H_2O + CO$. The identification of products in irradiated CH_3OH and $H_2O + CH_3OH$ ices, relevant to both IS and cometary ices, was discussed by Hudson and Moore [52]. Table 3 lists products we have identified in several simple ice mixtures after irradiation and photolysis.

Many of the mid-IR identifications discussed in this paper required appropriate reference spectra. Since no published library of spectra of relevant molecules in polar and/or non-polar ice matrices is available, we have created a spectral reference set of molecules in H_2O-dominated ices at 15–20 K measured from 4000 cm^{-1} (2.5 μm) to 400 cm^{-1} (25 μm) at 4 cm^{-1} resolution. It includes the following: carbon oxides CO, CO_2; alkanes CH_4, C_2H_6, C_3H_8, C_4H_{10}; alkenes C_2H_4, C_3H_6; alkynes C_2H_2, C_3H_4; dienes C_3H_4, C_4H_6; alcohols CH_3OH, C_2H_5OH; aldehydes H_2CO, CH_3COH; ketones $(CH_3)_2CO$, $(CH_3)(C_2H_5)CO$; acids HCOOH, CH_3COOH; ethers $(CH_3)_2O$, c-C_2H_4O; esters $HCOOCH_3$; amines NH_3, CH_3NH_2; assorted N_2O, HCN, H_2O_2, OCS. Spectral files are available at: www-691.gsfc.nasa.gov/cosmic_ices.

Confirming the identity of radiation products can be done in separate experiments using isotopically-labeled molecular components. A good example of this is our recent identification of the formate ion, $HCOO^-$, in irradiated $H_2O + CH_3OH$ ices. This identification was made by matching both the position and relative intensity of a feature near 1589 cm^{-1} and bands at 1384 and 1353 cm^{-1} with similar features in irradiated

Table 3
A comparison of products identified after proton irradiation or UV photolysis for several binary icy mixtures relevant to IS molecular clouds

Initial mixture	Products identified after proton irradiation or UV photolysis[a]
H_2O+CO	CO_2, HCO, H_2CO, CH_4(?), CH_3OH, HCOOH, **H_2CO_3**, **$HCOO^-$**
H_2O+CO_2	H_2CO_3, CO, CO_3, O_3, H_2O_2
H_2O+CH_3OH	CO_2, CO, HCO, H_2CO, CH_4, **$HCOO^-$**, $C_2H_4(OH)_2$
H_2O+CH_4	CO_2, CO, C_2H_6, C_2H_4, CH_3OH, C_2H_5OH, H_2CO, CH_3CHO, C_3H_8

[a] Products in bold-face are detected only in ion-irradiated ices.

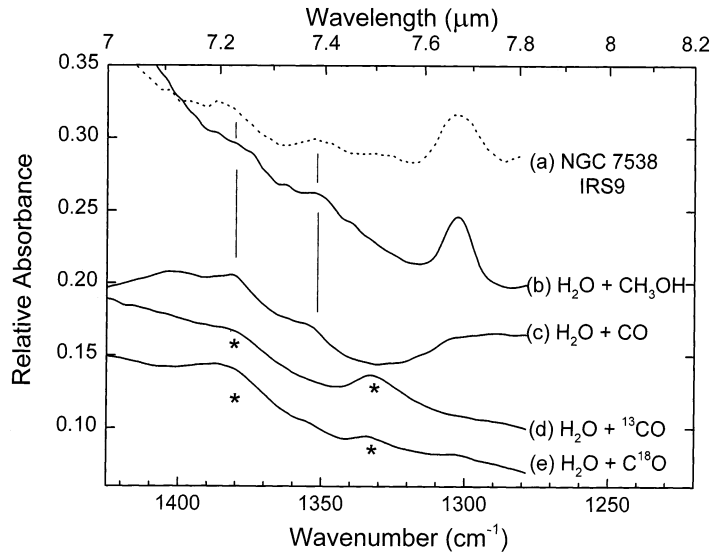

Fig. 8. $HCOO^-$ is detected at 1384 and 1353 cm^{-1} in irradiated water-dominated ices containing CH_3OH (b) or CO (c). Confirmation of this identification comes from isotope studies to form $H^{13}COO^-$ (d) and $HC^{18}OO^-$ (e). Spectra (b) and (c) match features observed by ISO in NGC 7538 IRS9 (a).

$H_2O + CO$. The $H_2O + CO$ features were identified as $HCOO^-$ through separate radiation experiments with $H_2O + {}^{13}CO$ and $H_2O + C^{18}O$ to form $H^{13}COO^-$ and $HC^{18}OO^-$, respectively. Fig. 8 compares the CH in-plane bending mode and CO stretching mode of the formate ion in the 1425 to 1300 cm^{-1} region. Spectra (b) and (c) show the similarity between the features in irradiated $H_2O + CH_3OH$ and $H_2O + CO$ at ~ 20 K. Features for $H_2O + CO$ are at 1381 and 1354 cm^{-1}. Spectrum (d) shows that the features in irradiated $H_2O + {}^{13}CO$ at 1381 and 1331 cm^{-1} are shifted 0 and 23 cm^{-1}, respectively, from the ^{12}CO position (expected shifts are 0 and 23 cm^{-1} [53]). Spectrum (e) shows that the features in irradiated $H_2O + C^{18}O$ at 1381 and 1334 cm^{-1} are shifted 0 and 20 cm^{-1}, respectively, from $C^{16}O$ (expected shifts are 2 and 20 cm^{-1} [53]).

Fig. 8(a) shows the ISO spectrum of NGC 7538 IRS 9 in the 7.5 μm region. A pair of features near 1384 and 1353 cm^{-1} appear similar to those in our irradiated $H_2O + CH_3OH$ and $H_2O + CO$ ices. We suggest [52] that $HCOO^-$ may be present in this and other IS ices, and may be a marker of CO or CH_3OH radiation processing in similar protostellar regions. Another identification of $HCOO^-$ in ices has involved acid-base reactions during warming $H_2O + HCOOH + NH_3$ [54] and $H_2O + HCOOH + N_2H_4$ [55].

3.5. Laboratory studies of H_2O_2 formation on Europa

Our study of H_2O_2 formation in irradiated 80 K ice was motivated by observations of this molecule on Europa [12]. An outline of our experiments is presented here as an example of how a combination of IR measurements, encompassing many of the techniques we have discussed, can be used to investigate such a problem. Hydrogen peroxide was identified on Europa, one of Jupiter's icy satellites, based on a 3.5 μm absorption feature in spectra obtained by the Galileo's near infrared mapping spectrometer[12]. Carlson et al. [12] matched the position and width of the observed IR feature with a laboratory reflectance spectrum of $H_2O + H_2O_2$ ice, where the H_2O_2 concentration was 0.13% by number relative to H_2O. The dominant ice on Europa H_2O is at a temperature near 100 K, and receives a constant flux of energetic ions from the Jovian magnetosphere. H_2O_2 was suggested by Carlson et al. [12]

since it is a radiation product consistent with early X- and γ-ray experiments on H_2O. We examined the conditions of H_2O_2 formation and detection at 3.5 μm in irradiated H_2O maintained at 80 K.

Simulation of Europa's icy surface and radiation environment in the laboratory involved H_2O ice films at 80–100 K, irradiated with MeV protons simulating different exposure times. We measured the IR reference spectrum of $H_2O + H_2O_2$ (100:1.4) at 16 K and determined $A(H_2O_2) = 2.7 \times 10^{-17}$ cm mol^{-1} for the 3.5 μm band [13]. Fig. 9a shows the spectrum of H_2O in the 3.5 μm region before and after irradiation at 16 K. H_2O_2 was detected on the wing of the H_2O band at 3.49 μm. The experiment was repeated at 80 K, but no H_2O_2 was detected after irradiation (Fig. 9b). Radiolysis of mixtures of H_2O with O_2 and with CO_2 did produce H_2O_2 at 80 K (Fig. 9c). CO_2 and O_2 are relevant to Europa since CO_2 has been detected on the surface of Europa and O_2 is found in its tenuous atmosphere. Formation mechanisms were suggested for H_2O_2 and these were supported by a variety of isotope studies (Moore and Hudson [13]). It is possible that destruction mechanisms for H_2O_2 in pure H_2O are more efficient at 80 K. The addition of O_2 to the ice increases the amount of H_2O_2 detected since H atom addition to O_2 can form H_2O_2 with little difficulty. The addition of CO_2 to the ice raises the abundance of H_2O_2, since CO_2 is an effective electron scavenger. Spectra of the H_2O_2 band formed in 80 K irradiated H_2O containing O_2 and CO_2 are shown in Fig. 9c and are compared with the observed Europan spectrum [12].

4. Summary

IR spectroscopy plays a major role in identifying new products in astrophysically relevant icy mixtures after UV photolysis and/or ion irradiation. In addition, spectroscopy may be used to monitor the stability of products at different temperatures. Identification is often based on a combination of techniques; matching an unknown spectral feature with appropriate reference spectra and performing relevant isotope experiments. We have placed TRT reference spectra of a variety of molecules in H_2O-dominated ice mixtures at 20 K at: http://www-691.gsfc.nasa.gov/cosmic_ices.

An important feature of recorded spectra is that the integrated absorbance value for IR bands of condensed-phase molecules, along with information about thickness, composition and ice density, can be used to calculate an intrinsic band strength, A. A-values are required to calculate the rate of formation and destruction of molecules during processing. Formation rates in UV-photolyzed and ion-processed ices can be compared to determine if one form of processing is more

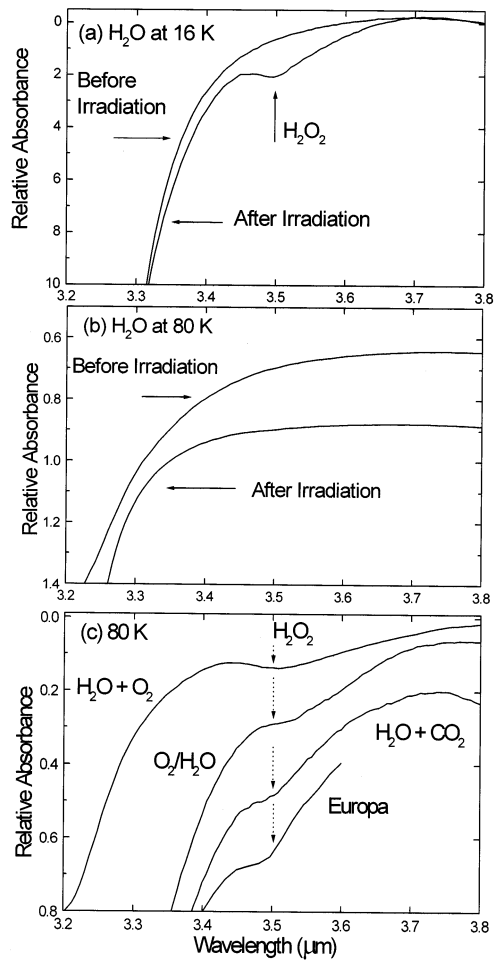

Fig. 9. Comparison of irradiated H_2O at 10 K (a) and 80 K (b) shows H_2O_2 does not form at 80 K in pure H_2O. H_2O_2 formation is detected after irradiation at 80 K if O_2, or CO_2 is present in the H_2O ice, or when O_2 exists on the surface of H_2O (O_2/H_2O).

effective than the other. Formation and destruction rates are also used to predict abundances in similarly processed cosmic ices.

Many IR studies have focused on H_2O, the dominant molecule in most cosmic environments. Far-IR spectroscopy can be used to identify the phase of H_2O ice. Since the 44 and 62 μm bands of crystalline H_2O shift position with temperature, the observation of their band location (or the ratio of their peak intensities) can be used as a thermometer for astronomical ices. Our laboratory far-IR H_2O spectra (available at: http://www-691.gsfc.nasa.gov/cosmic_ices) can be fitted to far-IR observations; matched band shapes can determine the H_2O ice phase and band positions can be a clue to the cosmic ice temperature.

Processing in laboratory experiments is thought to be representative of processes in space in spite of limited information about appropriate UV and ion radiation doses. Although the majority of absorption features detected in IS ices can be fitted with the spectrum of unprocessed ices, features at 4.6 and 6.8 μm in several IS sources may be markers of UV and/or ion (cosmic ray) processing. Evidence also exists for cosmic ray and/or UV processing in comet Hyakutake and ion (magnetospheric ions) processing on Europa's icy surface.

A quantitative comparison between ion bombardment and UV photolysis experiments for several H_2O-dominated mixtures containing CO_2, CH_3OH, or CH_4 shows that the formation rate of most major products is the same, independent of the energy source; e.g. the yield of H_2CO_3 and CO in UV-photolyzed and ion-bombarded $H_2O + CO_2$ is the same. However, one difference was found — the $HCOO^-$ radical is identified in proton-irradiated ices and not in those processed by UV-photolysis. Future experiments will compare the formation rate of products in ices containing N_2 and CO.

A recent example of the application of laboratory studies to astronomical observations is our work on H_2O_2 formation in 80 K water ices relevant to Europa. It is expected that future observations by space-based telescopes, such as SIRTF, NGST, or the IR spectrometer onboard the Saturn-bound Cassini spacecraft, may provide spectra of icy objects of higher quality than currently available. It is possible that spectroscopic evidence for the presence of complex organics may be found. A challenge will be simulating new icy environments in laboratory experiments, understanding any new identifications and possibly identifying less abundant species in both laboratory and astronomical spectra.

Acknowledgements

NASA funding through RTOPS 344-33-01 and 344-02-57 is acknowledged by the authors. RLH also acknowledges the support of NASA through grant NAG-5-1843 and of Eckerd College for a research leave to complete this work under an IPA agreement. This work was performed while PAG held an NRC-NASA/GSFC Research Associateship. Claude Smith and Steve Brown of the NASA/Goddard Radiation Facility are thanked for assistance with the irradiations. We thank Bernard Schmitt for sharing details of his laboratory far-IR data on H_2O ice and Rens Waters for sharing unpublished ISO observations and analyses of far-IR spectra of H_2O ice.

References

[1] R. Grim, J.M. Greenberg, Ap. J. 321 (1987) L91.
[2] K. Demyk, E. Dartois, L. d'Hendecourt, M. Jourdain de Muizon, A.M. Heras, M. Breitfellner, Astron. Astrophys. 339 (1998) 553.
[3] Y.J. Pendleton, A.G.G.M. Tielens, A.T. Tokunaga, M.P. Bernstein, Ap. J. 513 (1999) 294.
[4] R. Grim, J.M. Greenberg, W. Schutte, B. Schmitt, Ap. J. 341 (1989) L87.
[5] W.A. Schutte, A.G.G.M. Tielens, D.C.B. Whittet, A. Boogert, P. Ehrenfreund, T.H. de Graauw, T. Prusti, E.F. van Dishoeck, P. Wesselius, Astron. Astrophys. 315 (1996) L333.
[6] P.A. Gerakines, D.C.B. Whittet, P. Ehrenfreund, A.C.A. Boogert, A.G.G.M. Tielens, W.A. Schutte, J.E. Chiar, E.F. van Dishoeck, T. Prusti, F.P. Helmich, T.H. de Graauw, Ap. J. 522 (1999) 357.
[7] P. Ehrenfreund, O. Kerkhof, W.A. Schutte, A.C.A. Boogert, P.A. Gerakines, E. Dartois, L. d'Hendecourt, A.G.G.M. Tielens, E.F. van Dishoeck, D.C.B. Whittet, Astron. Astrophys. 350 (1999) 240.

[8] P. Ehrenfreund, A.C.A. Boogert, P.A. Gerakines, A.G.G.M. Tielens, E.F. van Dishoeck, Astron. Astrophys. 328 (1997) 649.
[9] M.J. Mumma, M.A. DiSanti, N. Dello Russo, M. Fomenkova, K. Magee-Sauer, C.D. Kaminski, D.X. Xie, Science 272 (1996) 1310.
[10] M.H. Moore, R.L. Hudson, Icarus 135 (1998) 518.
[11] R.L. Hudson, M.H. Moore, Icarus 126 (1997) 233.
[12] R.W. Carlson, M.S. Anderson, R.E. Johnson, W.D. Smythe, A.R. Hendrix, C.A. Barth, L.A. Soderblom, G.B. Hansen, T.B. McCord, J.B. Dalton, R.N. Clark, J.H. Shirley, A.C. Ocampo, D.L. Matson, Science 283 (1999) 2062.
[13] M.H. Moore, R.L. Hudson, Icarus 145 (2000) 282.
[14] B. Schmitt, E. Quirico, F. Trotta, W.M. Grundy, Optical properties of ices, in: B. Schmitt, C. de Bergh, M. Festov (Eds.), Solar System Ices, Kluwer Academic Pub, Dordrecht, 1998, p. 199.
[15] M.H. Moore, The Physics and Chemistry of Ices in the Interstellar Medium, in: L. d'Hendecourt, C. Joblin, A. Jones (Eds.), Solid Interstellar Matter: The ISO Revolution, EDP Sciences and Springer-VerlagInterstellar Matter, 1999, p. 199.
[16] F.F.S. van der Tak and E.F. van Dishoeck, Astron. Astrophys., submitted (2000).
[17] G. Strazzulla, R.E. Johnson, Irradiation effects on comets and cometry debris, in: R.L. Newburn, Jr, M. Neugebauer, J. Rahe (Eds.), Comets in the Post-Halley Era, Kluwer Academic Pub, 1991, p. 243.
[18] H. Okabe, Photochemistry of Small Molecules, Wiley, New York, 1978.
[19] P. Jenniskens, G.A. Baratta, A. Kouchi, M.S. de Groot, J.M. Greenberg, G. Strazzulla, Astron. Astrophys. 273 (1993) 583.
[20] T.J. Wdowiak, in: E. Bussoletti, G. Strazzulla (Eds.), Solid-State Astrophysics, Elsevier Science Pub, New York, 1991, p. 281.
[21] W.W. Duley, D.A. Williams, in: W.W. Duley, D.A. Williams (Eds.), Interstellar Chemistry, Academic Press, London, 1984, p. 7.
[22] J.F. Cooper, R.E. Johnson, B.H. Mauk, H.B. Garrett, N. Gehrels, Icarus, submitted (2000).
[23] A.G.G.M. Tielens, D.C.B. Whittet, Ices in Star Forming Regions, in: E.F. van Dishoeck (Ed.), Molecules in Astrophysics: Probes and Processes, IAU, 1997, p. 45.
[24] W.M. Grundy, M.W. Buie, J.A. Stansberry, J.R. Spencer, Icarus 142 (1999) 546.
[25] J.K. Davies, T.L. Roush, D.P. Cruikshank, M.J. Bartholomew, T.R. Geballe, T. Owen, C. de Bergh, Icarus 127 (1997) 238.
[26] E.L. Gibb, D.C.B. Whittet, W.A. Schutte, A.C.A. Boogert, J.E. Chiar, P. Ehrenfreund, P.A. Gerakines, J.V. Keane, A.G.G.M. Tielens, E.F. van Dishoeck, O. Kerkhof, Ap. J., 536 (2000) 347.
[27] J. Crovisier, Faraday Discuss. 109 (1998) 437.
[28] D. Cruikshank, R.H. Brown, W.M. Calvin, R.L. Roush, M.J. Bartholomew, Ices on the Satellites of Jupiter, Saturn and Uranus, in: B. Schmitt, C. De Bergh, M. Festou (Eds.), Solar System Ices, Kluwer Academic Pub, Dordrecht, 1998, p. 579.
[29] M.H. Moore, R.F. Ferrante, J.A. Nuth, III, et al., Planet. Space Sci. 44 (1996) 927.
[30] R.L. Hudson, M.H. Moore, Rad. Phys. Chem. 45 (1995) 779.
[31] P.A. Gerakines, M.H. Moore, R.L. Hudson, Astron. Astrophys. 357 (2000) 793.
[32] D.M. Hudgins, S.A. Sandford, L.J. Allamandola, Ap. J. Suppl. Ser. 86 (1993) 713.
[33] R.G. Smith, G. Robinson, A.R. Hyland, G.L. Carpenter, Mon. Not. R. Astron. Soc. 271 (1994) 481.
[34] L.C. Northcliffe, R.F. Shilling, Nuclear Data Tables A7 (1970) 233.
[35] P. Warneck, Appl. Opt. 1 (6) (1962) 721.
[36] E. Dartois, P. Cox, P.R. Roelfsema, A.P. Jones, A.G.G.M. Tielens, L. d'Hendecourt, M. Jourdain de Muizon, B. Schmitt, T. Lim, B. Swinyard, A.M. Heras, Astron. Astrophys. 338 (1998) L21.
[37] L.B.F.M. Waters private communication (2000).
[38] M.H. Moore, R.L. Hudson, Astron. Astrophys. Suppl. Ser. 103 (1993) 45.
[39] A. Coustenis, B. Schmitt, R.D. Khanna, F. Trotta, Planet. Space Sci. 47 (1999) 1305.
[40] J.E. Bertie, H.J. Labbe, E. Whalley, J. Phys. Chem. 50 (1969) 4501.
[41] M.H. Moore, R.K. Khanna, Spectrochim. Acta 47A (2) (1991) 255.
[42] A.C.A. Boogert, W.A. Schutte, E.P. Helmich, A.G.G.M. Tielens, D.H. Wooden, Astron. Astrophys. 317 (1997) 929.
[43] D.A. Dows, Spectrochim. Acta 22 (1966) 1479.
[44] G.J. Jiang, W.B. Person, K.G. Brown, J. Chem. Phys. 64 (1975) 2101.
[45] H. Yamada, W.B. Person, J. Chem. Phys. 41 (1964) 2478.
[46] P.A. Gerakines, W.A. Schutte, J.M. Greenberg, E.F. van Dishoeck, Astron. Astrophys. 296 (1995) 810.
[47] L.J. Allamandola, S.A. Sandford, G.J. Valero, Icarus 76 (1988) 225.
[48] S.A. Sandford, L.J. Allamandola, A.G.G.M. Tielens, G.J. Valero, Astrophys. J. 329 (1988) 498.
[49] T.Y. Brooke, A.T. Tokunaga, H.A. Weaver, J. Crovisier, D. Bockelée-Morvan, D. Crisp, Nature 383 (1996) 606.
[50] H.A. Weaver, T.Y. Brooke, G. Chin, S.J. Kim, D. Bockelée-Morvan,J.K. Davies, in First International Conference on Comet Hale-Bopp, Tenerife, Canary Islands, 1998.
[51] R.L. Hudson, M.H. Moore, Icarus 140 (1999) 451.
[52] R.L. Hudson, M.H. Moore, Icarus 145 (2000) 661.
[53] E. Spinner, J.E. Rowe, Aust. J. Chem. 32 (1979) 481.
[54] W.A. Schutte, A.C.A. Boogert, A.G.G.M. Tielens, D.C.B. Whittet, P.A. Gerakines, J.E. Chiar, P. Ehrenfreund, J.M. Greenberg, E.F. van Dishoeck, Th. de Graauw, Astron. Astrophys., 343 (1999) 966.
[55] N. Boudin, W.A. Schutte, J.M. Greenberg, Astron. Astrophys. 331 (1998) 749.